Fault Detection for Solar Thermal Systems - Overall System Evaluation or Component-Oriented Approach

Christoph Schmelzer[1], Matthias Georgii[1], Janybek Orozaliev[1] and Klaus Vajen[1]

[1] Institute of Thermal Engineering, University of Kassel, Kassel (Germany)

Abstract

The paper at hand describes an FSC-based method to automatically assess the performance of a solar combi system. The impact of both inexpensive and improved sensor equipment on the detection accuracy is investigated, capabilities and limitations of this approach are discussed. Advantages and disadvantages of this overall system evaluation are compared to those of the standard fault detection system by means of a component-oriented approach.

Keywords: Solar heating, yield control, function control, monitoring, fault detection

1. Overall System Evaluation – FSC-based approach

This section gives a short overview of the Fractional Solar Consumption (FSC) in application to assessing the performance of a solar combi system. More details on the capabilities and limitations of this approach can be found in (Schmelzer et. al. 2018, Georgii et. al. 2019).

The overall system evaluation is based on FSC, which was developed in IEA SHC task 26 to compare solar combi systems with different system designs at different locations in Europe (Letz, 2002). The underlying principle is illustrated in fig. 1: to determine the maximum solar fraction, the usable solar radiation (orange dashed area) is divided by the reference demand (green + orange dashed area). The usable solar radiation is calculated by comparing the radiation on the collector plane and the measured heat demand (with estimated storage losses), taking into account that solar excess radiation in summer cannot be used.

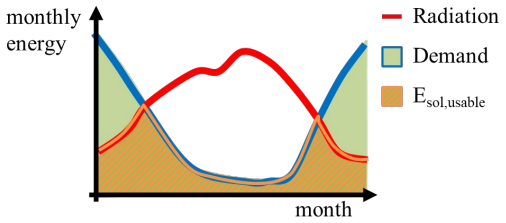

Fig. 1: Comparison of monthly energy demand and solar radiation to determine the maximum usable solar energy for a specific building, dhw demand, collector area, slope and tilt (Letz, 2002)

FSC does not depend on any system design aspects (except the collector area), but on the total irradiation on the collector plane and the demand. Therefore, it describes the energetic boundary conditions for the system. To calculate FSC, the heat demand for domestic hot water Q_{dhw} (incl. circulation) and space heating Q_{sh} must be measured. Since the storage in solar heating systems is larger compared to a reference system, the storage losses for the reference $Q_{loss,ref}$ are estimated using eq. 1. The equation considers a storage size of 75 % of the daily dhw draw-off.

$$Q_{loss,ref} = 0.16 \frac{\mathrm{W}}{\mathrm{K}} \sqrt{0.75 \cdot \left(\frac{\mathrm{l}}{\mathrm{d}}\right)^{-1} \cdot V_{dhw,daily}} \cdot (52.5 - 15)\mathrm{K} \cdot \Delta t \qquad \text{(eq. 1)}$$

With these losses, the reference energy E_{ref} can be calculated as follows:

$$E_{ref} = Q_{dhw} + Q_{sh} + Q_{loss,ref}. \qquad \text{(eq. 2)}$$

As described above, the usable solar energy is calculated as sum of monthly minima of the irradiation on the collector plane $\left(A_{col} \cdot H_{t,m}\right)$ and the heat demand E_{ref} for the whole year:

$$E_{sol,usable} = \sum_{m=1}^{12} \min\left[\left(A_{col} \cdot H_{t,m}\right), E_{ref,m}\right]. \qquad \text{(eq. 3)}$$

The FSC is then calculated by dividing the usable solar energy by the reference energy demand:

$$FSC = \frac{E_{sol,usable}}{E_{ref}}. \qquad \text{(eq. 4)}$$

doi:10.18086/eurosun.2020.04.02 Available at http://proceedings.ises.org

There are some minor differences to the standard calculation approach described in (Letz, 2002). For simplicity, no boiler efficiencies were taken into account. In eqs. 2-4 only delivered energies are considered.

To assess the systems performance, another key figure describing the actual system behaviour is needed. In the following, this is done by a slightly adjusted definition of the fractional solar savings f_{sav}. Normally, boiler efficiencies and a (simulated) reference for the auxiliary energy are required to calculate f_{sav}. By assuming that the boiler efficiencies are almost the same and estimating the storage losses according to eq. 1, f_{sav} can be calculated as follows:

$$f_{sav} = 1 - \frac{Q_{aux,delivered}}{E_{ref}} . \qquad \text{(eq. 5)}$$

In (Letz, 2002) quadratic correlations are used to describe the relation between the expected f_{sav} (for fault free systems) and FSC. In the present approach power functions are chosen (see eq. 6), which enable the correction of several influential parameters (Georgii et. al. 2009).

$$f_{sav,expected} = e^{c_0} \cdot (FSC)^{c_{FSC}} \cdot (X_1)^{c_1} \cdot (X_2)^{c_2} \cdot (X_3)^{c_3} \cdot \ldots \qquad \text{(eq. 6)}$$

The underlying system simulations and the subsequent analysis showed that the following parameter must be considered for a reliable prediction of f_{sav}:

- Share of Q_{dhw} in $E_{sol,usable}$
- Ratio of auxiliary heated storage volume to daily dhw draw-off
- UA-value of the storage
- Specific storage volume (l/m²$_{coll}$)
- Boiler setpoint temperature

With the described set of formulas, the systems performance can be assessed automatically by calculating the measured energy savings $f_{sav,measured}$ (eq. 5) and comparing them to the expected savings $f_{sav,expected}$ for the fault-free system operation, using eq. 6. Fig. 2 illustrates the general principle.

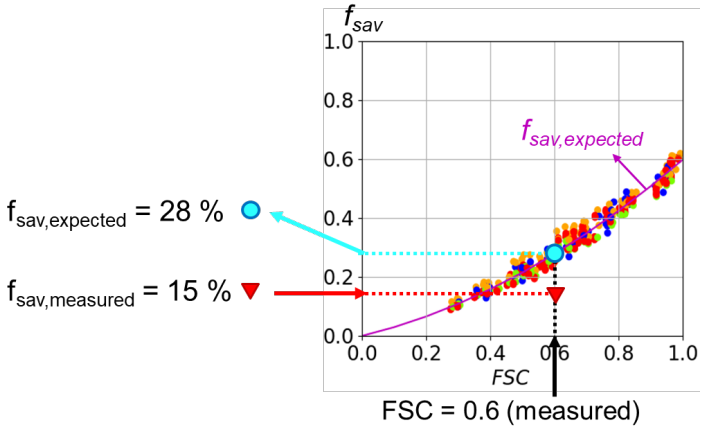

Fig. 2: System assessment with FSC – 1. Calculate $f_{sav,measured}$ with measured auxiliary energy – 2. Calculate $f_{sav,expected}$ using FSC correlations

Thus, the performance indicator PI can be calculated:

$$PI = \frac{f_{sav,measured}}{f_{sav,expected}} . \qquad \text{(eq. 7)}$$

With this easy-to-understand key figure, the system performance can directly be evaluated. The performance indicator can theoretically detect any fault with a significant impact on the solar energy yield.

2. Impact of measurement uncertainties on detection accuracy of FSC-based overall system evaluation

2.1 Methodology – Monte Carlo Analysis

To estimate the impact of different sensor equipment on the accuracy of the key figures and calculate respective uncertainties, a Monte Carlo Analysis (MCA) was performed. To do so, sensor data, previously modelled by simulations, was used as the true value of each sensor and then uncertainties were added as follows.

In the first step, the systematic sensor uncertainties u_{sys} are chosen normally distributed and independent of each other. The standard deviation for the normal distribution σ is set to be a half of the measurement uncertainty of the respective sensor (X):

$$\sigma = \frac{u_{X,sys}}{2}. \qquad \text{(eq. 8)}$$

This approach ensures that 95.5 % of the selected uncertainties lie within the specified limits. Conversely, this also means that 4.5 % of the measurement errors exceed the limits and show larger deviations. As an example, fig. 3 illustrates three different fixed systematic errors for a sensor measuring temperature or temperature difference. The 2σ range [-0.8K, 0.8K] is marked in magenta. Three specific systematic uncertainties each fixed for one calculation run, are depicted by blue, green and cyan arrows. The mean of the normal distribution is chosen at 0 K, meaning that randomly chosen uncertainties are most likely much smaller than the specified limit. However, there is a small probability of 4.5%, that the randomly chosen value exceeds the 2σ range, e.g. the cyan arrow in fig. 3. At the end of step one, each signal gets shifted by its offset (fig. 4, left).

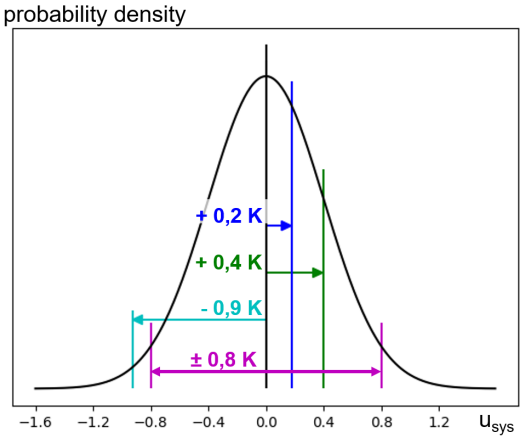

Fig. 3: MCA – Exemplary selection of systematic uncertainties for temperature or temperature difference measurement

In the second step, normally distributed stochastic noise is applied to the data (with a standard deviation equal to half of the maximum error of each sensor and the mean value equal to zero), see fig. 4, right.

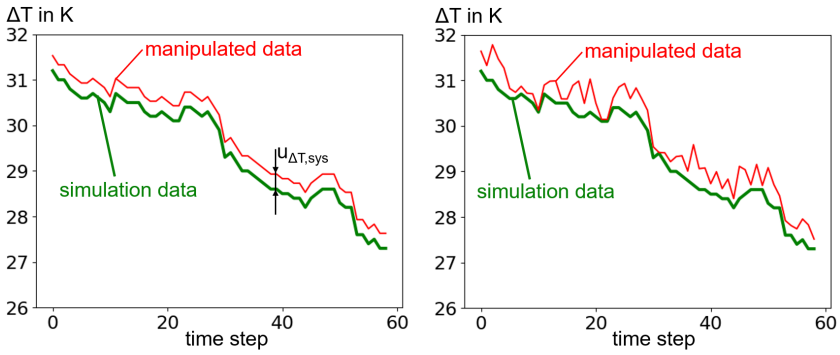

Fig. 4: MCA – Exemplary selection of systematic uncertainty (shift on the left) and stochastic noise (on the right) for a temperature difference

Finally, the monthly energies and key figures are calculated using sensor data manipulated in two previous steps.

To obtain reliable probability distributions for the system key figures, it is required by the MCA to repeat these three steps very often (in this paper n = 1,000 times). In this way, a large number of randomly selected systematic uncertainties is taken into account. From the distributions 68 % and 95.5 % quantiles can be derived, which can be used as a measure for the resulting uncertainties for f_{sav} and FSC. In the following, the 95.5 % quantiles are used.

2.2 Impact of inexpensive sensor equipment on detection accuracy

Since the additional costs are crucial for the implementation of a fault detection system, first step was to investigate

the impact of an inexpensive reference measurement equipment on the fault detection accuracy. The reference sensor equipment consists of the following sensors:

- Temperature sensors: Class B
- Flow measurement: Vortex Sensors (accuracy ± 5 % RD)
- Radiation: Estimated via satellite data

Fig. 5 illustrates the resulting uncertainties for f_{sav} and FSC for one example system and their impact on the detection accuracy of the system evaluation. The black circle shows the actual f_{sav}-FSC-value for one specific combi system in Germany with a collector area of 20 m². As displayed by the red error bars, the key figures cannot be determined very precisely. The actual f_{sav} = 34 % and FSC = 66 % can only be roughly estimated due to inaccuracy of the sensor equipment at the following ranges: f_{sav} = (22..46) %, FSC = (57..75) %.

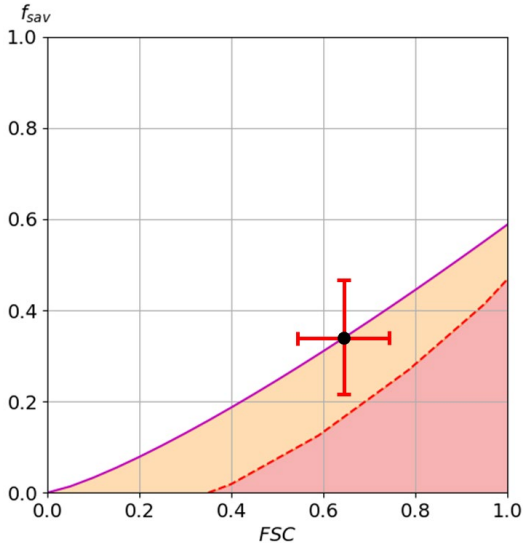

Fig. 5: Impact of inexpensive sensor equipment on detection accuracy

Moreover, the uncertainties have a strong impact on the detection accuracy and on the informative value of the system assessment. The orange area in fig. 5 illustrates the resulting uncertainties for the correlation. The dotted red line shows the minimum f_{sav} for systems with this measurement equipment, that still might be close to the theoretical correlation. Only if the measured f_{sav} lies within the red area it is certain, that there must be a fault in the system causing a detectable reduced energy yield. This also means that the fault detection is not possible where the red area is zero. Thus, for the inexpensive sensor equipment, the detection is only applicable for systems with f_{sav} > 18 % or an FSC > 35 %.

2.3 Cost-efficient measurement equipment

To reduce measurement uncertainties and therewith enhance detection accuracy, a cost-efficient solution must be found. Based on an extensive market research, costs for different sensors were identified (end user prices for Germany incl. VAT and installation). Then, each sensor was improved separately and the effect on f_{sav} and FSC was analysed. In this way, the most influential sensors can be determined and reasonable sensor combinations for improving the detection accuracy identified. A detailed analysis of the effects of single sensors on the measured heat quantities in each loop can be found in (Schmelzer et. al. 2019). Fig. 6 shows the resulting costs and uncertainties. On the y-axis the improved uncertainties of f_{sav} and FSC are divided by the uncertainty of the reference sensor equipment, see 2.2. On the x-axis costs of different sensor improvements are shown. Starting with the reference sensor equipment at total costs of approx. 1,000€, the first step is replacing the temperature sensors in the auxiliary and space heating loops by class AA sensors. In the second step, additionally, the dhw temperature sensors are improved to class AA sensors, water meters are placed in aux and sh loop and a radiation sensor is installed. Steps 3, 4 and 5 show the additional impact of heat meters in different loops.

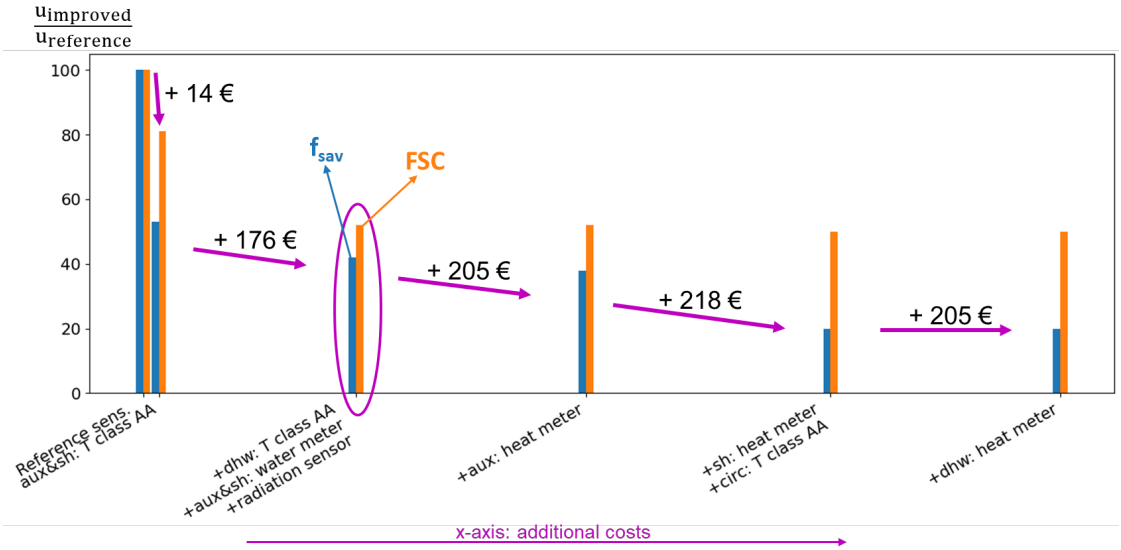

Fig. 6: Costs for improving sensor accuracy and impact on uncertainty of resulting key figures f_{sav} and FSC

As fig.6 illustrates, the first two steps have the largest impact on uncertainty of both key figures, while still being reasonably priced. For additional 190 €, the uncertainties of f_{sav} and FSC can be reduced by 60 % and 50 %, respectively. In the further steps it can be seen that a heat meter in the auxiliary loop does not reduce the uncertainties noticeably, but a heat meter in the space heating loop has a significant impact on the accuracy of f_{sav}. Since the heat meter price (incl. installation) is about 200 €, application of heat meters is not considered in the following. To show the impact of an improved sensor equipment, the second step is chosen as the improved set of sensors (magenta ellipse in fig.6, improved: T class AA in aux, sh and dhw loops; water meter in aux and sh loops; radiation sensor).

2.4 Impact of improved sensor equipment

Fig. 7 illustrates the impact of the improved sensors on the uncertainty ranges for f_{sav} and FSC (green error bars) compared to the inexpensive reference equipment (red error bars). With the improved sensors the resulting uncertainty ranges of the example system are reduced significantly: The actual values of f_{sav} = 34 % and FSC = 66 % can be estimated at the following ranges: f_{sav} = (30..38) %, FSC = (61..71) %.

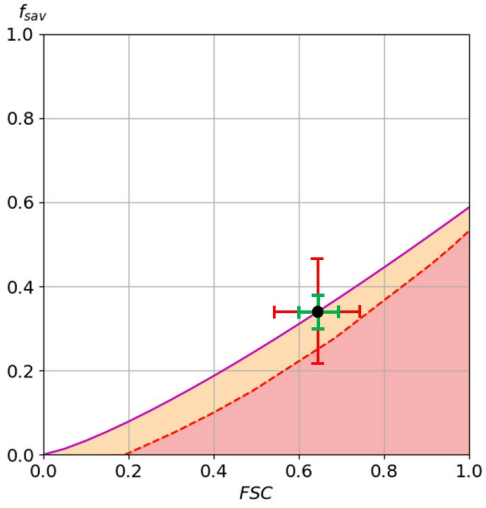

Fig. 7: Impact of improved sensor equipment on detection accuracy

The uncertainty range for the system assessment is also significantly reduced by this improvement. As fig. 7 shows, the yellow area is much narrower compared to the reference (see fig. 5). This means that the fault detection is possible for systems with a mean or predicted f_{sav} > 10 % and FSC > 20 %. Thus, the fault detection is applicable for a much wider variety of combi systems. Tab. 1 summarises the results of different sensor equipment.

Tab. 1: Impact of inexpensive and improved sensor equipment on system assessment

	Additional costs (approx.)	Uncertainty range of f_{sav} and FSC for example system	No assessment for systems with a mean f_{sav} or FSC if
Reference sens. equipment	1,000 €	f_{sav} = (34 ± 12) % FSC = (65 ± 8) %	f_{sav} < 18 % FSC < 35 %
Improved sens. equipment	1,200 €	f_{sav} = (34 ± 4) % FSC = (65 ± 5) %	f_{sav} < 10 % FSC < 20 %

3. Component-Oriented Approach

Instead of aiming at the most universal and powerful fault indicator, another approach is to make use of the already existing measurement equipment and to investigate, which information regarding the functionality of the STS can be derived. Often, this approach focuses on the assessment of single components rather than on the evaluation of the whole system. Fig. 8 shows a stepwise approach for an algorithm-based, component-oriented fault detection. In the first step, measured values are combined to generate features, e.g. a flow sensor can be used to calculate the feature “loop in operation” if the measured flow is above a specified threshold. If a feature or a combination of features reveal unusual or unexpected behaviour, a symptom is generated. E.g. if the temperatures in the solar loop are very high during operation. In the last step, faults in the system can be diagnosed or at least narrowed down by analysing the occurring symptoms.

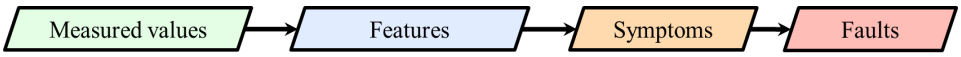

Fig. 8: Stepwise approach for an algorithm-based, component-oriented fault detection

To develop algorithms for a specific fault, first the suspicious system behaviour (symptom) which points to this fault must be identified. On this basis, different detection paths can be investigated and tested with measured or simulated data. Depending on the required sensors, paths with low or no additional costs can be identified. E.g., if the pump in the solar loop stops working, this could easily be detected with a flow sensor, which, however, is usually not installed in small STS. One symptom related to this fault is, that no temperature difference between flow and return side is expected, even when the operation conditions are met (fig. 9). The operation conditions can be checked by the controller’s pump signal (feature in magenta). The feature in cyan is an indicator for pump operation generated by using the flow and return temperatures only. In this STS, a valve in the solar loop was closed between 18th and 21st May 2016 to simulate a pump failure. As fig. 9 shows, the described symptom is reliably reported (green/red) on the days where the pump failure is simulated.

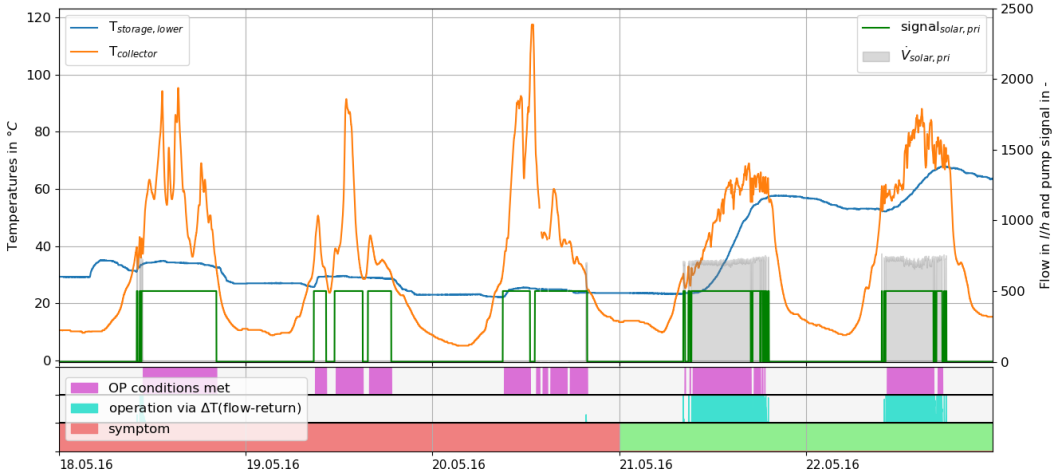

Fig. 9: Features and symptom for a pump failure detection, using controller signal and temperatures

4. Conclusion and comparison

The capabilities and limitations of the discussed approaches are summarised and compared in Tab. 2. On the one hand, the main advantage of the FSC-based overall system evaluation is its comprehensibility and, at the same time, simplicity of the PI indicator: the output describes the whole system and it can be understood without any background knowledge. Moreover, this approach automatically detects faults whenever the fractional solar savings f_{sav} are significantly reduced. Therefore, so the approach is reliable and automatically rates faulty states according to their impact on the energy savings, thus avoiding "unimportant" faults. On the other hand, the approach is only applicable for larger combi systems and has high additional costs of about 1,200 € because of the required precise measurement equipment. The FSC-based system assessment does not provide information on the possible cause for the reduced f_{sav}, and since 12 months of data are required to calculate the key figures, the reaction time is rather slow.

The component-oriented approach on the contrary addresses exactly these challenges. It is applicable for basically any system and reacts directly to faults that can be detected by available measurement equipment at no additional costs. Since the algorithms must be designed for specific faults or symptoms (suspicious system behaviour), the informative value of the output is much higher. However, often a component's behaviour must be derived indirectly, taking into account its interactions with other components. Hence, the prior information is required or (implicit) assumptions have to be made about a component's surrounding, i.e. to which other components it is linked, and which other signals are available. This means that it is much effort to take into account many different possibilities for both the surroundings of a component and the available measurement equipment, even when looking at just one fault or symptom. This has a negative impact on the level of automation and the comprehensibility of the delivered output. Instead of a single intuitive key figure, the different algorithms generate symptoms and create warnings if the system behaves unusually. These messages have to be "manually" analysed by the user or by sophisticated subsequent algorithms which still have to be developed. Additionally, it must be noted, that the capabilities and limitations for the algorithm-based approach significantly depend on the existing or planned measurement equipment. Starting with basic equipment at no additional costs, only few algorithms will be applicable and, thus, few faults detectable. If an extensive system assessment is to be implemented, the additional costs will increase.

Tab. 2: Comparison of Overall System Evaluation and Component-Oriented Approach

	Overall System Evaluation (FSC-based approach)	**Component-oriented approach (algorithm-based)**
Easy to understand	+	-
Reliable (no false alarms)	+	-
Automated	+	+
Low costs	-	+
Informative (what is wrong)	-	+
Applicable for any system	-	+
Response time	-	+

For larger solar combi systems, application of both approaches is recommended. In this way the assessment can benefit from the additional information and the fast response time of the algorithm-based approach on the one hand, and from the automated rating of the energetic impact of any fault on the other hand. For smaller solar assisted heating systems and other applications, the component-oriented, algorithm-based approach is still the only applicable option and should hence be considered early in the planning phase. It can be very beneficial, if additional (inexpensive) sensors are implemented in strategic places to enable the applicability of as many algorithms as possible.

Acknowledgments

We would like to thank the German Federal Ministry for Economic Affairs and Energy BMWi (FKZ 0325870A) and the PtJ, our scientific partners CEA INES, IGTE Stuttgart, and our project partners Bosch, Enertracting, RESOL, SOLVIS, Vaillant, Viessmann, and WILO.

References

Letz, T., 2002. Validation and background information on the FSC procedure. A Report of IEA SHC Task 26 – Solar Combisystems. URL: https://task26.iea-shc.org/Data/Sites/1/publications/task26-b-dc_procedure.pdf (last accessed 29.08.2020)

Georgii M., Schmelzer C., Kusyy O., Orozaliev J., Vajen K., 2019. Zur Verbesserung der Abschätzung der Leistungsfähigkeit thermischer Solaranlagen mittels FSC-Korrelationen. Proc. Symposium Solarthermie, Bad Staffelstein, 21.05.-23.05.2019

Schmelzer C., Georgii M., Kusyy O., Orozaliev J., Vajen K., 2018. Towards Automated Continuous Performance Benchmarking of DHW and Combi Systems. Proc. EuroSun, Rapperswil, Switzerland, 10.09.-13.09.2018. doi:10.18086/eurosun2018.01.10, URL: http://proceedings.ises.org/paper/eurosun2018/eurosun2018-0019-Schmelzer.pdf (last accessed 31.08.2020)

Schmelzer C., Georgii M., Kusyy O., Orozaliev J., Vajen K., 2019. Auswirkungen von Messunsicherheiten auf die Genauigkeit der Ermittlung von Wärmemengen in solarunterstützten Wärmeversorgungssystemen. Proc. Symposium Solarthermie, Bad Staffelstein, 21.05.-23.05.2019